SIAM J. NUMER. ANAL.
Vol. 55, No. 1, pp. 144–167

NUMERICAL SOLUTION OF DIFFRACTION PROBLEMS: A HIGH-ORDER PERTURBATION OF SURFACES AND ASYMPTOTIC WAVEFORM EVALUATION METHOD*

DAVID P. NICHOLLS†

Abstract. The rapid and robust simulation of linear waves interacting with layered periodic media is a crucial capability in many areas of scientific and engineering interest. High-order perturbation of surfaces (HOPS) algorithms are interfacial methods which recursively estimate scattering quantities via perturbation in the interface shape heights/slopes. For a single incidence wavelength such methods are the most efficient available in the parameterized setting we consider here. In the current contribution we generalize one of these HOPS schemes by incorporating a further expansion in the wavelength about a base configuration which constitutes an "asymptotic waveform evaluation" (AWE). We not only provide a detailed specification of the algorithm, but also verify the scheme and point out its benefits and shortcomings. With numerical experiments we show the remarkable efficiency, fidelity, and high-order accuracy one can achieve with an implementation of this algorithm.

Key words. high-order perturbation of surfaces methods, asymptotic waveform evaluation, high-order spectral methods, Helmholtz equation, diffraction gratings, layered media

AMS subject classifications. 65N35, 78A45, 78B22

DOI. 10.1137/16M1059679

1. Introduction.

The rapid and robust simulation of linear waves interacting with layered periodic media (a diffraction or scattering problem) is a crucial capability in many areas of scientific and engineering interest. Examples abound in areas such as geophysics [VO09, BR09], oceanography [BL82], materials science [God92], imaging [NW01], and nanoplasmonics [Rae88, Mai07, EB12]. For this latter topic, one can investigate topics as diverse as extraordinary optical transmission [ELG98], surface enhanced spectroscopy [Mos85], and surface plasmon resonance (SPR) biosensing [Hom08, ILW11] and [LJJ12, JJJ13, RJOM13, NRJO14]. Regardless of the physical problem, in each it is necessary to approximate the scattering returns of such models in a fast, highly accurate, and reliable fashion.

While all of the classical numerical algorithms have been utilized for simulation of this problem, we have recently argued [AN14, Nic16, Nic15, NOJR16] that such *volumetric* approaches (such as finite differences and finite/spectral element methods) are greatly disadvantaged with an unnecessarily large number of unknowns for the layered media problems we consider here. Interfacial methods based upon integral equations (IEs) [CK98] are a natural candidate but, as we have pointed out [AN14, Nic16, Nic15, NOJR16], these also face difficulties. Most of these have been addressed in recent years through (i) the use of sophisticated quadrature rules to deliver high-order spectral accuracy, (ii) the design of preconditioned iterative solvers with suitable acceleration [GR87], and (iii) new strategies to avoid periodizing the Green function [BG11, CB15, LKB15]. Consequently, they are a compelling alternative (see, e.g., the survey article of [RT04] for more details); however, two properties render them

*Received by the editors February 2, 2016; accepted for publication (in revised form) September 9, 2016; published electronically January 24, 2017.
http://www.siam.org/journals/sinum/55-1/M105967.html
Funding: This work was supported by the National Science Foundation through grant DMS–1522548.
†Department of Mathematics, Statistics, and Computer Science, University of Illinois at Chicago, Chicago, IL 60607 (davidn@uic.edu).

noncompetitive for the *parameterized* problems we consider as compared with the methods we advocate here:

1. For configurations parameterized by the real value ε (for us the height/slope of the irregular interface), an IE solver will return the scattering returns only for a particular value of ε. If this value is changed then the solver must be run again.
2. The dense, nonsymmetric positive definite systems of linear equations which must be inverted with each simulation.

As we advocated in [Nic16, Nic15, NOJR16] a "high-order perturbation of surfaces" (HOPS) approach can effectively address these concerns. More specifically, in [Nic15, NOJR16] we argued for the method of field expansions (FE) which trace their roots to the low-order calculations of Rayleigh [Ray07] and Rice [Ric51]. Their high-order incarnation was first introduced by Bruno and Reitich [BR93a, BR93b, BR93c] and later enhanced and stabilized by the author and Reitich [NR04a, NR04b, NR08], and the author and Malcolm [MN11]. These formulations are particularly compelling as they maintain the advantageous properties of classical IE formulations (e.g., surface formulation and exact enforcement of far-field and quasi-periodicity conditions) while avoiding the shortcomings listed above:

1. Since the methods are built upon expansions in the boundary parameter, ε, once the Taylor coefficients are known for the scattering quantities, it is simply a matter of summing these (rather than beginning a new simulation) for any given choice of ε to recover the returns.
2. Due to the perturbative nature of the scheme, at every perturbation order one need only invert a single, sparse operator corresponding to the flat-interface, order-zero approximation of the problem.

For a *single* incidence wavelength such methods are the most efficient available in the parameterized setting we consider here. We now discuss a generalization of the HOPS approach of Bruno and Reitich which incorporates a further expansion in the wavelength about a base configuration that constitutes an "asymptotic waveform evaluation" (AWE) [PR90, KSN96, RDCB98, SLL01]. We will not only provide a detailed specification of the algorithm, but also verify the scheme and point out its benefits and shortcomings. With numerical experiments we shall show the remarkable efficiency, fidelity, and high-order accuracy one can achieve with an implementation of this algorithm. In this initial contribution we will defer several natural generalizations to focus upon the idea of the algorithm rather than solving all possible problems. In section 6 we discuss several of these future directions including three-dimensional geometries and vectorial scattering (section 6.1), frequency-dependent materials (section 6.2), and the occurrence of Rayleigh singularities [Ray07] (section 6.3). We note that these singularities are commonly referred to as "Wood's anomalies," but we encourage the interested reader to find the fascinating article of Maystre in Chapter 1 of [EB12] which argues that this term is, in fact, a misnomer. Beyond this we note that nothing about our algorithm limits the configuration to two layers and, up to notational complications, the developments of [MN11, Nic12, NRJO14, AN14, Nic15, Nic16] could be extended, which we intend to complete in a forthcoming publication.

The paper is organized as follows: In section 2 we briefly recall the equations which govern the propagation of linear waves in a two-dimensional periodic structure, and in section 2.1 we recall the Rayleigh expansions. In section 3 we recall the FE method for numerically approximating solutions to these governing equations, together with the Taylor expansions necessary to specify an implementation (in section 3.1). In section 4 we describe in some detail our new HOPS/AWE algorithm, including forms

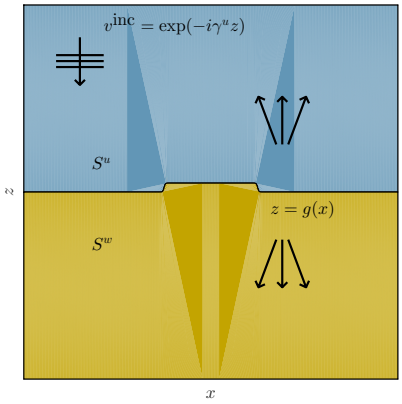

FIG. 1. *Plot of two–layer structure with periodic interface.*

for the Taylor terms required of the algorithm in sections 4.1 and 4.2. In section 5 we present detailed numerical results (see sections 5.1–5.5) to validate our implementation versus exact solutions, the previously tested FE recursions, and a boundary IE (BIE) simulation [CB15]. These illustrate the accuracy and computational efficiency of our new method, the latter of which we make precise in section 5.6. In section 6 we give concluding remarks and discuss future directions.

2. The governing equations. The geometry we consider is displayed in Figure 1: a y-invariant, doubly layered structure. Dielectrics occupy both domains, one (with refractive index n^u) fills the region *above* the graph $z = g(x)$,

$$S^u := \{z > g(x)\},$$

while the other (with index of refraction n^w) fills

$$S^w := \{z < g(x)\}.$$

The superscripts are chosen to conform to the notation of previous work by the author [NOJR16, NT16, Nic12]. The grating is d-periodic so that $g(x + d) = g(x)$. The structure is illuminated from above by monochromatic plane-wave incident radiation of frequency ω and wavenumber $k^u = n^u\omega/c_0 = \omega/c^u$ (c_0 is the speed of light), aligned with the grooves. We consider the reduced incident fields

$$\mathbf{E}^{inc}(x,z) = \mathbf{A}e^{i\alpha x - i\gamma^u z}, \quad \mathbf{H}^{inc}(x,z) = \mathbf{B}e^{i\alpha x - i\gamma^u z},$$
$$\alpha = k^u \sin(\theta), \quad \gamma^u = k^u \cos(\theta),$$

where time dependence of the form $\exp(-i\omega t)$ has been factored out. The reduced electric and magnetic fields $\{\mathbf{E}, \mathbf{H}\}$, like the reduced scattered fields, are α-quasi-periodic due to the incident radiation [Pet80]. To close the problem, we specify that the scattered radiation is "outgoing" (upward propagating in S^u and downward propagating in S^w).

It is well-known (see, e.g., Petit [Pet80]) that in this two-dimensional setting, the time-harmonic Maxwell equations decouple into two scalar Helmholtz problems which govern the transverse electric (TE) and transverse magnetic (TM) polarizations. We define the invariant (y) directions of the scattered (electric or magnetic) fields by $\{u(x,z), w(x,z)\}$ in S^u and S^w, respectively, and the incident radiation in the upper

layer by $u^{inc}(x,z)$. For all three we factor out the phase factor $\exp(i\alpha x)$ leaving functions d-periodic in the x direction.

In light of all of this, we are led to seek outgoing, d-periodic solutions of

$$\begin{aligned}
&\Delta u + (2i\alpha)\partial_x u + (\gamma^u)^2 u = 0, && z > g(x), \quad \text{(1a)}\\
&\Delta w + (2i\alpha)\partial_x w + (\gamma^w)^2 w = 0, && z < g(x), \quad \text{(1b)}\\
&u - w = \zeta, && z = g(x), \quad \text{(1c)}\\
&\partial_N u - (i\alpha)(\partial_x g)u - \tau^2\left\{\partial_N w - (i\alpha)(\partial_x g)w\right\} = \psi, && z = g(x), \quad \text{(1d)}
\end{aligned}$$

where the Dirichlet and Neumann data are

$$\zeta(x) := -e^{-i\gamma^u g(x)}, \quad \psi(x) := \left(i\gamma^u + i\alpha(\partial_x g)\right) e^{-i\gamma^u g(x)}.$$

In these $N = (-\partial_x g, 1)^T$ and

$$\tau^2 = \begin{cases} 1, & \text{TE},\\ (k^u/k^w)^2 = (n^u/n^w)^2, & \text{TM}, \end{cases}$$

where $\gamma^w = k^w\cos(\theta)$. For various reasons the case of TM polarization is of extraordinary importance (e.g., the classical study of SPRs [Rae88]) and thus we concentrate our attention on the TM case from here.

2.1. The Rayleigh expansions. The Rayleigh expansions, which can be derived from separation of variables [Pet80], are the periodic, outgoing solutions of (1a) and (1b). More specifically, they express the fields as

$$u(x,z) = \sum_{p=-\infty}^{\infty} \hat{a}_p e^{i\tilde{p}x} e^{i\gamma_p^u z}, \quad w(x,z) = \sum_{p=-\infty}^{\infty} \hat{d}_p e^{i\tilde{p}x} e^{-i\gamma_p^w z}, \tag{2}$$

where, for $p \in \mathbf{Z}$ and $q \in \{u, w\}$,

$$\tilde{p} := \left(\frac{2\pi}{d}\right) p, \quad \alpha_p := \alpha + \tilde{p}, \quad \gamma_p^q := \begin{cases} \sqrt{(k^q)^2 - \alpha_p^2}, & p \in \mathcal{U}^q,\\ i\sqrt{\alpha_p^2 - (k^q)^2}, & p \notin \mathcal{U}^q, \end{cases}$$

and

$$\mathcal{U}^q = \left\{ p \in \mathbf{Z} \mid \alpha_p^2 < (k^q)^2 \right\},$$

which are the "propagating modes" in the upper and lower layers. Notice that $\hat{a}_p$ and $\hat{d}_p$ are the upward and downward propagating Rayleigh amplitudes. Quantities of great interest are the *efficiencies*

$$e_p^u = (\gamma_p^u/\gamma^u)\left|\hat{a}_p\right|^2, \quad e_p^w = (\gamma_p^w/\gamma^u)\left|\hat{d}_p\right|^2,$$

which give the "reflectivity map"

$$R := \sum_{p \in \mathcal{U}^u} e_p^u. \tag{3}$$

3. Field expansions. Before we discuss our new algorithm, we review the classical HOPS methodology due to Bruno and Reitich, the "FE method" [BR93a, BR93b, BR93c]. Our viewpoint is that the FE algorithm is a perturbative approach to enforcing the boundary conditions (1c) and (1d) with the $\{\hat{a}_p, \hat{d}_p\}$ from the Rayleigh expansions (2) as unknowns.

For this we define

$$a(x) := u(x,0) = \sum_{p=-\infty}^{\infty} \hat{a}_p e^{i\tilde{p}x}, \quad d(x) := w(x,0) = \sum_{p=-\infty}^{\infty} \hat{d}_p e^{i\tilde{p}x}, \tag{4}$$

which are the "flat interface" field traces. We recall the definition of a Fourier multiplier, $m(D)$,

$$m(D)\xi(x) := \sum_{p=-\infty}^{\infty} m(p)\hat{\xi}_p e^{i\tilde{p}x},$$

where $\hat{\xi}_p$ is the pth Fourier coefficient of $\xi(x)$. With this we can define the Fourier multipliers

$$U := i\gamma_D^u, \quad W := i\gamma_D^w, \quad A := i\alpha_D, \tag{5}$$

where the final operator is simply classical differentiation of a α-quasi-periodic function. Now, follow [Nic15, NOJR16] and define the Dirichlet trace operators

$$\mathcal{D}^u : a \to u(x, g(x)), \quad \mathcal{D}^w : d \to w(x, g(x)),$$

and their Neumann counterparts

$$\mathcal{N}^u : a \to \left(\partial_z u - (\partial_x g)\partial_x u\right)(x, g(x)), \quad \mathcal{N}^w : d \to \left(\partial_z w - (\partial_x g)\partial_x w\right)(x, g(x)).$$

These operators map, respectively, the function pair (a, d) to the upper and lower Dirichlet and Neumann traces. It can be shown [Nic15, NOJR16] that these operators have the form

$$\mathcal{D}^u = \exp(gU), \quad \mathcal{D}^w = \exp(-gW), \tag{6a}$$

and

$$\begin{aligned} \mathcal{N}^u &= \exp(gU)U - (\partial_x g)\exp(gU)A, \\ \mathcal{N}^w &= -\exp(-gW)W - (\partial_x g)\exp(-gW)A. \end{aligned} \tag{6b}$$

To clarify, we note that the meaning of $\mathcal{D}^u$ is given by

$$\mathcal{D}^u[\xi] = \sum_{p=-\infty}^{\infty} \exp(g(x)i\gamma_p^u)\hat{\xi}_p e^{i\tilde{p}x}.$$

In terms of these, the Dirichlet boundary condition, (1c), becomes

$$\mathcal{D}^u[a] - \mathcal{D}^w[d] = \zeta, \tag{7}$$

while the Neumann condition, (1d), becomes

$$\mathcal{N}^u[a] - (i\alpha)(\partial_x g)\mathcal{D}^u[a] - \tau^2\left\{\mathcal{N}^w[d] - (i\alpha)(\partial_x g)\mathcal{D}^w[d]\right\} = \psi. \tag{8}$$

We state our *governing equations*, the boundary conditions (7) and (8), abstractly as

$$\mathbf{M}\mathbf{v} = \mathbf{b}, \tag{9}$$

where

$$\mathbf{M} = \begin{pmatrix} \mathcal{D}^u & -\mathcal{D}^w \\ \mathcal{N}^u - (i\alpha)(\partial_x g)\mathcal{D}^u & -\tau^2\left\{\mathcal{N}^w - (i\alpha)(\partial_x g)\mathcal{D}^w\right\} \end{pmatrix}, \quad \mathbf{v} = \begin{pmatrix} a \\ d \end{pmatrix}, \quad \mathbf{b} = \begin{pmatrix} \zeta \\ \psi \end{pmatrix}.$$

3.1. Taylor expansions. The FE methodology considers interface deformations of the form $g(x) = \varepsilon f(x)$ ($f = \mathcal{O}(1)$) and notes that, for f sufficiently smooth (Lipschitz) and ε sufficiently small, the linear operator $\mathbf{M}$ and inhomogeneity $\mathbf{b}$ are both analytic in ε [NR01, NR03]. Furthermore, an analytic solution $\mathbf{v}$ can be shown to exist so that the following Taylor expansions are convergent:

$$\{\mathbf{M}, \mathbf{v}, \mathbf{b}\}(\varepsilon f) = \sum_{n=0}^{\infty} \{\mathbf{M}_n(f), \mathbf{v}_n(f), \mathbf{b}_n(f)\}\varepsilon^n.$$

The FE approach recovers $\mathbf{v}_n$ using regular perturbation theory. To see this we write (9) as

$$\left(\sum_{n=0}^{\infty} \mathbf{M}_n \varepsilon^n\right)\left(\sum_{\ell=0}^{\infty} \mathbf{v}_\ell \varepsilon^\ell\right) = \sum_{n=0}^{\infty} \mathbf{b}_n \varepsilon^n,$$

and, equating at each perturbation order, we find

$$\mathbf{M}_0 \mathbf{v}_n = \mathbf{b}_n - \sum_{\ell=0}^{n-1} \mathbf{M}_{n-\ell}\mathbf{v}_\ell. \tag{10}$$

At order zero we recover the flat-interface solution, giving the Fresnel coefficients, while higher-order corrections, $\mathbf{v}_n$, can be computed by appealing to (10). Of great importance is the fact that one only need invert the *same* linear operator, $\mathbf{M}_0$ at *every* perturbation order. All that remains is a specification of the terms $\{\mathbf{M}_n, \mathbf{b}_n\}$.

Regarding the Dirichlet trace operators, upon defining

$$F_n(x) := f(x)^n/n!,$$

it has been shown that [Nic15, NOJR16]

$$\mathcal{D}_n^u = F_n U^n, \quad \mathcal{D}_n^w = F_n(-W)^n.$$

For their Neumann counterparts we have

$$\mathcal{N}_n^u = F_n U^{n+1} - (\partial_x f)F_{n-1}U^{n-1}A, \quad \mathcal{N}_n^w = F_n(-W)^{n+1} - (\partial_x f)F_{n-1}(-W)^{n-1}A.$$

Finally, for the surface data, $\mathbf{b}_n$, it is easy to show that

$$\zeta_n = -F_n\left(-i\gamma^u\right)^n$$

and

$$\psi_n = F_n\left(i\gamma^u\right)\left(-i\gamma^u\right)^n e^{i\alpha x} + (\partial_x f)F_{n-1}\left(i\alpha\right)\left(-i\gamma^u\right)^{n-1},$$

where $F_{-1}(x) \equiv 0$ and $F_0(x) \equiv 1$. To clarify, we note that the meaning of $\mathcal{D}_n^u$ is given by

$$\mathcal{D}_n^u[\xi] = \frac{f(x)^n}{n!} \sum_{p=-\infty}^{\infty} (i\gamma_p^u)^n \hat{\xi}_p e^{i\tilde{p}x}.$$

4. A HOPS/AWE approach. To describe our new HOPS/AWE method we recall the governing equations, (7)–(8),

$$\begin{aligned}
&\mathcal{D}^u\left[a\right]-\mathcal{D}^w\left[d\right]=\zeta,\\
&\mathcal{N}^u\left[a\right]-(i\alpha)(\partial_x g)\mathcal{D}^u\left[a\right]-\tau^2\left\{\mathcal{N}^w\left[d\right]-(i\alpha)(\partial_x g)\mathcal{D}^w\left[d\right]\right\}=\psi,
\end{aligned}$$

which we wrote compactly as $\mathbf{M}\mathbf{v}=\mathbf{b}$; c.f. (9). We now make two smallness assumptions:

1. Boundary perturbation: $g(x)=\varepsilon f(x)$, $\varepsilon\in\mathbf{R}$, $\varepsilon\ll 1$.
2. Frequency perturbation: $\omega=(1+\delta)\underline{\omega}=\underline{\omega}+\delta\underline{\omega}$, $\delta\in\mathbf{R}$, $\delta\ll 1$.

(We suspect that more careful analysis will reveal that neither ε nor δ need be infinitesimal for our method to be applicable.) We note that the latter of these has a number of consequences:

$$\begin{aligned}
k^u&=\omega/c^u=(1+\delta)\underline{\omega}/c^u=:(1+\delta)\underline{k}^u=\underline{k}^u+\delta\underline{k}^u,\\
k^w&=\omega/c^w=(1+\delta)\underline{\omega}/c^w=:(1+\delta)\underline{k}^w=\underline{k}^w+\delta\underline{k}^w,\\
\alpha&=k^u\sin(\theta)=(1+\delta)\underline{k}^u\sin(\theta)=:\underline{\alpha}+\delta\underline{\alpha},\\
\gamma^u&=k^u\cos(\theta)=(1+\delta)\underline{k}^u\cos(\theta)=:\underline{\gamma}^u+\delta\underline{\gamma}^u,\\
\gamma^w&=k^w\cos(\theta)=(1+\delta)\underline{k}^w\cos(\theta)=:\underline{\gamma}^w+\delta\underline{\gamma}^w.
\end{aligned}$$

These in turn imply

$$\alpha_p=\alpha+(2\pi/d)p=\underline{\alpha}+\delta\underline{\alpha}+(2\pi/d)p=:\underline{\alpha}_p+\delta\underline{\alpha}.$$

Akin to the FE method outlined above, we will assume for the moment the *joint* analyticity of the operator $\mathbf{M}$ and inhomogeneity $\mathbf{b}$ with respect to *both* boundary and frequency deviations. With these we postulate that the *joint* analyticity of $\mathbf{v}$ can be established so that the following Taylor series can be shown to be convergent:

$$\{\mathbf{M},\mathbf{v},\mathbf{b}\}(\varepsilon f,\underline{\omega}+\delta\underline{\omega})=\sum_{n=0}^{\infty}\sum_{m=0}^{\infty}\{\mathbf{M}_{n,m}(f,\underline{\omega}),\mathbf{v}_{n,m}(f,\underline{\omega}),\mathbf{b}_{n,m}(f,\underline{\omega})\}\varepsilon^n\delta^m.$$

It is a goal of future research to make this mathematically precise. Our new HOPS/AWE algorithm finds the $\mathbf{v}_{n,m}$ at each perturbation order using regular perturbation theory. Now we write (9) as

$$\left(\sum_{n=0}^{\infty}\sum_{m=0}^{\infty}\mathbf{M}_{n,m}\varepsilon^n\delta^m\right)\left(\sum_{\ell=0}^{\infty}\sum_{r=0}^{\infty}\mathbf{v}_{\ell,r}\varepsilon^\ell\delta^r\right)=\sum_{n=0}^{\infty}\sum_{m=0}^{\infty}\mathbf{b}_{n,m}\varepsilon^n\delta^m,$$

and, equating at each perturbation order, we find

$$\begin{aligned}
\mathbf{M}_{0,0}\mathbf{v}_{n,m}=\mathbf{b}_{n,m}&-\sum_{\ell=0}^{n-1}\mathbf{M}_{n-\ell,0}\mathbf{v}_{\ell,m}-\sum_{r=0}^{m-1}\mathbf{M}_{0,m-r}\mathbf{v}_{n,r}\\
&-\sum_{\ell=0}^{n-1}\sum_{r=0}^{m-1}\mathbf{M}_{n-\ell,m-r}\mathbf{v}_{\ell,r}.
\end{aligned}\tag{11}$$

As before, the key is to discover forms for the $\{\mathbf{M}_{n,m},\mathbf{b}_{n,m}\}$ and we now begin this process.

4.1. Expansions of γ_p^u, γ_p^w, U, and W in frequency. The first step in our development is to derive the Taylor series expansion for γ_p^q, $q \in \{u, w\}$,

$$\gamma_p^q = \gamma_p^q(\delta) = \sum_{m=0}^{\infty} \gamma_{p,m}^q \delta^m. \tag{12}$$

We begin by using the fundamental relationship

$$\alpha_p^2 + (\gamma_p^q)^2 = (k^q)^2,$$

which implies

$$\left(\sum_{m=0}^{\infty} \gamma_{p,m}^q \delta^m\right)\left(\sum_{r=0}^{\infty} \gamma_{p,r}^q \delta^r\right) = (1+\delta)^2 (\underline{k}^q)^2 - \left(\underline{\alpha}_p + \delta\underline{\alpha}\right)^2.$$

This delivers

$$\begin{aligned}\sum_{m=0}^{\infty} \delta^m \sum_{r=0}^{m} \gamma_{p,m-r}^q \gamma_{p,r}^q &= \left\{(\underline{k}^u)^2 - (\underline{\alpha}_p)^2\right\} + 2\delta\left\{(\underline{k}^q)^2 - \underline{\alpha}\ \underline{\alpha}_p\right\} + \delta^2\left\{(\underline{k}^q)^2 - (\underline{\alpha})^2\right\} \\ &= (\underline{\gamma}_p^u)^2 + 2\delta\left\{(\underline{k}^q)^2 - \underline{\alpha}\ \underline{\alpha}_p\right\} + \delta^2(\underline{\gamma}^q)^2,\end{aligned}$$

so that at order $\mathcal{O}(\delta^0)$ we require

$$\gamma_{p,0}^q = \pm\underline{\gamma}_p^q, \tag{13}$$

while at order $\mathcal{O}(\delta^1)$ we need

$$\gamma_{p,1}^q = \frac{2((\underline{k}^q)^2 - \underline{\alpha}\ \underline{\alpha}_p)}{2\gamma_{p,0}^q}, \quad \gamma_{p,0}^q \neq 0. \tag{14}$$

Here we now see that it is crucial for the validity of expansion (12) that $\underline{\gamma}_p^q \neq 0$ for *all* p. We now make this assumption, and report upon the case $\underline{\gamma}_p^q = 0$ for *some* p in section 6.3. Continuing our development to $\mathcal{O}(\delta^2)$ we further set

$$\gamma_{p,2}^q = \frac{(\underline{\gamma}^q)^2 - (\gamma_{p,1}^q)^2}{2\gamma_{p,0}^q}, \quad \gamma_{p,0}^q \neq 0, \tag{15}$$

and for $\mathcal{O}(\delta^m)$, $m > 2$, we demand

$$\gamma_{p,m}^q = \frac{-\sum_{r=1}^{m-1} \gamma_{p,m-r}^q \gamma_{p,r}^q}{2\gamma_{p,0}^q}, \quad \gamma_{p,0}^q \neq 0. \tag{16}$$

To close, recall the definitions of U, W, and A:

$$U = i\gamma_D^u, \quad W = i\gamma_D^w, \quad A = i\alpha_D;$$

c.f. (5). In light of our expansions for $\gamma^u(\delta)$ and $\gamma^w(\delta)$, we expand

$$\{U, W, A\} = \{U, W, A\}(\delta) = \sum_{m=0}^{\infty} \{U_m, W_m, A_m\}\delta^m, \tag{17}$$

and it is a simple matter to show that

$$U_m = i\gamma_{D,m}^u, \quad W_m = i\gamma_{D,m}^w, \quad A_m = \begin{cases} i\underline{\alpha}_D, & m = 0, \\ i\underline{\alpha}, & m = 1, \\ 0, & m > 1. \end{cases}$$

4.2. Expansion of the Dirichlet and Neumann trace operators. We are now in a position to find expressions for the Taylor series terms $\{\mathbf{M}_{n,m}, \mathbf{b}_{n,m}\}$ which require the forms $\{\mathcal{D}^u_{n,m}, \mathcal{D}^w_{n,m}, \mathcal{N}^u_{n,m}, \mathcal{N}^w_{n,m}\}$ from

$$\{\mathcal{D}^u, \mathcal{D}^w, \mathcal{N}^u, \mathcal{N}^w\} = \{\mathcal{D}^u, \mathcal{D}^w, \mathcal{N}^u, \mathcal{N}^w\}(\varepsilon, \delta) = \sum_{n=0}^{\infty}\sum_{m=0}^{\infty} \left\{\mathcal{D}^u_{n,m}, \mathcal{D}^w_{n,m}, \mathcal{N}^u_{n,m}, \mathcal{N}^w_{n,m}\right\} \varepsilon^n \delta^m. \tag{18}$$

It is clear from the formulas (6a)–(6b), if appropriate forms can be found for

$$\mathcal{E}^u := \exp(gU) = \exp(\varepsilon f U(\underline{\omega} + \delta\underline{\omega})) = \sum_{n=0}^{\infty}\sum_{m=0}^{\infty} \mathcal{E}^u_{n,m}\varepsilon^n\delta^m, \tag{19a}$$

$$\mathcal{E}^w := \exp(-gW) = \exp(-\varepsilon f W(\underline{\omega} + \delta\underline{\omega})) = \sum_{n=0}^{\infty}\sum_{m=0}^{\infty} \mathcal{E}^w_{n,m}\varepsilon^n\delta^m \tag{19b}$$

then

$$\mathcal{D}^u_{n,m} = \mathcal{E}^u_{n,m}, \quad \mathcal{D}^w_{n,m} = \mathcal{E}^w_{n,m},$$

while a little more work delivers

$$\mathcal{N}^u_{n,m} = \sum_{r=0}^{m} \mathcal{E}^u_{n,m-r}U_r - (\partial_x f)\mathcal{E}^u_{n-1,m}A_0 - (\partial_x f)\mathcal{E}^u_{n-1,m-1}A_1,$$

$$\mathcal{N}^w_{n,m} = -\sum_{r=0}^{m} \mathcal{E}^w_{n,m-r}W_r - (\partial_x f)\mathcal{E}^w_{n-1,m}A_0 - (\partial_x f)\mathcal{E}^w_{n-1,m-1}A_1.$$

In order to find the Taylor series terms for $\mathcal{E}^u$ we insert the expansion

$$U = U(\delta) = \sum_{m=0}^{\infty} U_m\delta^m$$

into (19a), and since

$$\mathcal{E}^u(0,\delta) = \exp(0\ U(\delta)) = I,$$

we have

$$\mathcal{E}^u_{0,m} = \begin{cases} I, & m = 0, \\ 0, & m > 0. \end{cases} \tag{20}$$

Next,

$$\mathcal{E}^u(\varepsilon, 0) = \exp(\varepsilon f U(0)) = \sum_{n=0}^{\infty} F_n U(0)^n,$$

so that

$$\mathcal{E}^u_{n,0} = F_n U(0)^n.$$

Finally, we follow the technique of Pourahmadi [Pou84] (see also the works of Roberts [Rob83] and Marchant and Roberts [MR87]) who uses the fact that

$$\partial_\varepsilon \mathcal{E}^u = f\mathcal{E}^u U,$$

to equate

$$\sum_{n=0}^{\infty}\sum_{m=0}^{\infty} \mathcal{E}^u_{n+1,m}(n+1)\varepsilon^n\delta^m = f\left(\sum_{n=0}^{\infty}\sum_{m=0}^{\infty}\mathcal{E}^u_{n,m}\varepsilon^n\delta^m\right)\left(\sum_{m=0}^{\infty}U_m\delta^m\right).$$

Upon equating at like orders we have

$$\mathcal{E}^u_{n+1,m} = \frac{f}{n+1}\sum_{r=0}^{m}\mathcal{E}^u_{n,m-r}U_r.$$

So, to discover the coefficient at order $(n+1,m)$, one only needs $(n,0),\ldots,(n,m)$. For instance, we have $\mathcal{E}^u_{0,m}$ from (20) which gives $\mathcal{E}^u_{1,m}$ and one can proceed to recover all of the $\mathcal{E}^u_{n,m}$. Clearly, the same procedure can be used to deduce that

$$\begin{aligned}
\mathcal{E}^w_{0,m} &= \begin{cases} I, & m=0,\\ 0, & m>0,\end{cases}\\
\mathcal{E}^w_{n,0} &= F_n(-W(0))^n,\\
\mathcal{E}^w_{n+1,m} &= -\frac{f}{n+1}\sum_{r=0}^{m}\mathcal{E}^w_{n,m-r}W_r.
\end{aligned}$$

5. Numerical results. We are now in a position to test a numerical implementation of this algorithm and demonstrate its advantageous computational complexity. For this we compare our novel HOPS/AWE method to the carefully studied and validated classical FE scheme of Bruno and Reitich [BR93a, BR93b, BR93c] outlined in section 3. Both the FE and our new HOPS/AWE schemes are high–order spectral approaches, where nonlinearities are approximated with convolutions implemented via the fast Fourier transform (FFT) algorithm [GO77, CHQZ88].

To demonstrate the convergence of our algorithm we take several steps as we feel it helps illuminate not only the accuracy of our new scheme, but also its range of validity. To begin we consider convergence of partial sums of the Taylor series for γ_p^u given in (12), and then move to approximation of the *operator* U by the partial sums of its Taylor series (17). We then proceed to study the convergence of partial Taylor sums of the Dirichlet and Neumann trace operators from (18). To close, of course, we consider computations of the full reflectivity map (3) from (10) or (11).

5.1. Approximation of $\boldsymbol{\gamma_p^u}$. To begin our demonstrations we recall that the frequency perturbation assumption

$$\omega = \omega(\delta) = \underline{\omega}(1+\delta)$$

led to the Taylor expansion of the quantity

$$\gamma_p^u = \gamma_p^u(\delta) = \sum_{m=0}^{\infty}\gamma^u_{m,p}\delta^m;$$

c.f. (12). Our numerical approximation will be to truncate this Taylor series after a finite number of terms,

$$\gamma_p^u(\delta) \approx \gamma_p^{u,M}(\delta) := \sum_{m=0}^{M} \gamma_{m,p}^u \delta^m \tag{21}$$

with forms for the $\gamma_{m,p}^u$ given in (13)–(16).

As we noted before, the expansion (12) ceases to be valid when $\underline{\gamma}_p^u = 0$ for *any* p which we term a "Rayleigh singularity" (commonly called a Wood's anomaly), and we now quantify what this means for our computations. Since

$$\underline{\alpha}_p^2 + (\underline{\gamma}_p^u)^2 = (\underline{k}^u)^2,$$

a singularity occurs when $\underline{\alpha}_p^2 = (\underline{k}^u)^2$ for any integer p (notice that this cannot occur for $p = 0$). To simplify matters we assume that

$$\alpha = 0, \quad d = 2\pi,$$

and recall that $\underline{k}^u = \underline{\omega}/c^u = n^u\underline{\omega}/c_0$ (where c_0 is the speed of light which we choose to be unity). In this case $\underline{\alpha}_p = p$ so that the Rayleigh singularity condition becomes, if $n^u = 1$ (vacuum),

$$p^2 = (\underline{k}^u)^2 = \underline{\omega}^2/(c^u)^2 = (n^u)^2\underline{\omega}^2 = \underline{\omega}^2.$$

Thus "resonance" occurs at *integer* values of the frequency $\underline{\omega}$. To maximize the radius of convergence of our algorithm in our tests we define

$$\underline{\omega}_q := q + \frac{1}{2}, \quad q = 0, 1, 2, 3, \ldots$$

and choose

$$\left(q + \frac{1}{2}\right) - \frac{\sigma}{2} < \omega(\delta) < \left(q + \frac{1}{2}\right) + \frac{\sigma}{2}$$

to sample at a fraction $0 < \sigma < 1$ of the "allowable" frequencies implying, after some simplification, that

$$-\frac{\sigma}{2q+1} < \delta < \frac{\sigma}{2q+1}.$$

In Figure 2 we display results of the comparison between a numerical implementation of the approximation $\gamma_p^{u,M}$ (c.f. (21)), versus an exact computation of γ_p^u. More specifically, we compute

$$\text{Error} := \frac{\max_{\{-N_x/2 \le p \le N_x/2-1\}} \left|\gamma_p^{u,M} - \gamma_p^u\right|}{\max_{\{-N_x/2 \le p \le N_x/2-1\}} \left|\gamma_p^u\right|} \tag{22}$$

for parameter choices

$$q = 1, \quad \sigma = 0.99, \quad n^u = 1, \quad N_x = 32, \quad M = 4, 8, 16, 32, 64$$

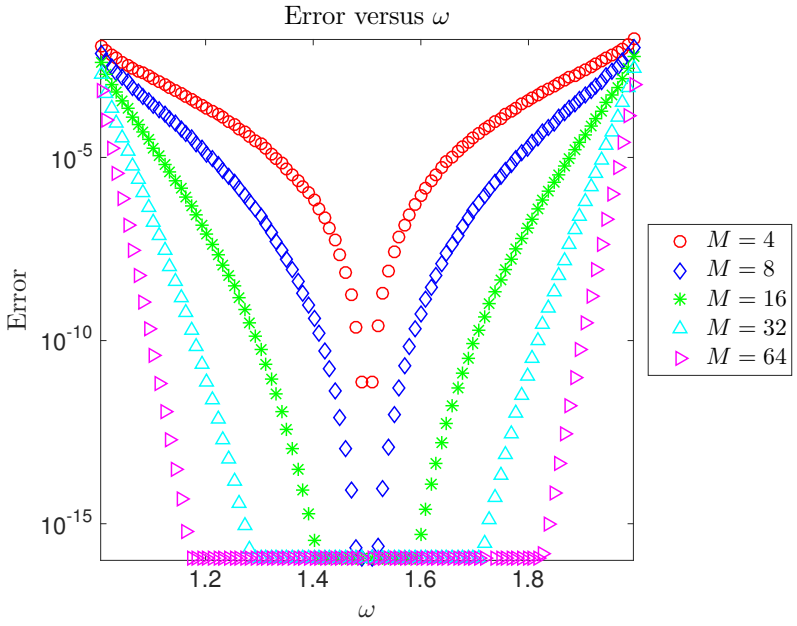

FIG. 2. *Relative maximum norm error,* (22)*, versus frequency* ω *in approximation of* γ_p^u *by* $\gamma_p^{u,M}$ $(-N_x/2 \le p \le N_x/2 - 1)$ *for various perturbation orders* M*. Parameter choices are* $q = 1$*,* $\sigma = 0.99$*,* $n^u = 1$*,* $N_x = 32$*, and* $M = 4, 8, 16, 32, 64$*.*

5.2. Approximation of U. We now repeat the computations from the previous section for the operator $U = U(\delta)$, the Fourier multiplier which has $i\gamma_p^u(\delta)$ as its symbol. As before, we will use the analyticity of U as a function of δ to approximate its action, beginning with

$$U = U(\delta) = \sum_{m=0}^{\infty} U_m \delta$$

(c.f. (17)); we will simulate U by truncating this series

$$U(\delta) \approx U^M(\delta) := \sum_{m=0}^{M} U_m \delta. \tag{23}$$

In section 4.1 we saw that the symbol of the Fourier multiplier U_m is given by $i\gamma_{p,m}^u$ so we may simply use the formulas (13)–(16) together with the FFT to approximate the action of U_m and thus U^M.

Figure 3 shows the outcomes of the comparison between a numerical implementation of the approximation U^M (c.f. (23)), versus an exact computation of U. More precisely, we compute (at N_x collocation points on $[0, 2\pi]$)

$$\text{Error} := \frac{\left|U^M[\xi] - U[\xi]\right|_{L^\infty}}{|U[\xi]|_{L^\infty}} \tag{24}$$

for

$$\xi(x) = e^{\cos(x)} + ie^{\sin(x)},$$

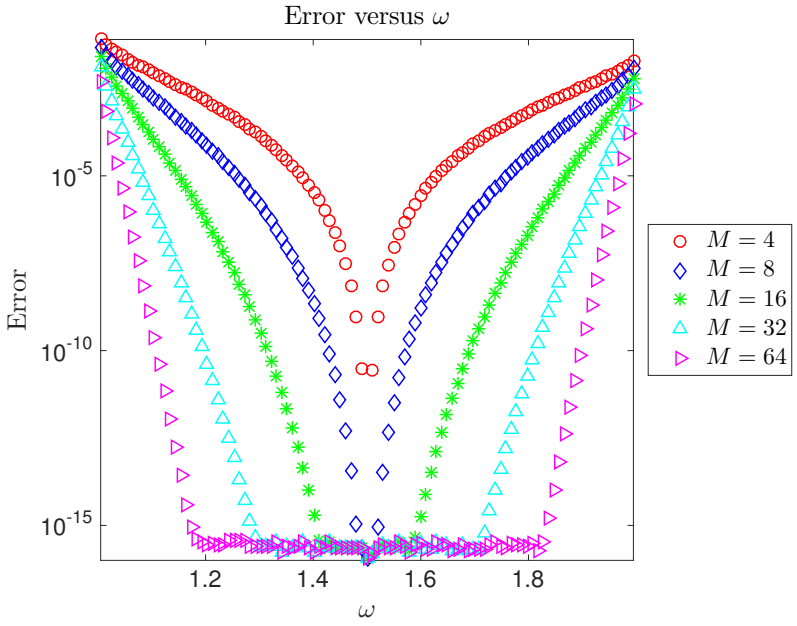

FIG. 3. *Relative supremum norm error,* (24)*, versus frequency* ω *in approximation of* U *by* U^M *for various perturbation orders* M*. Parameter choices are* $q = 1$*,* $\sigma = 0.99$*,* $n^u = 1$*,* $N_x = 32$*, and* $M = 4, 8, 16, 32, 64$*.*

and parameter choices

$$q = 1, \quad \sigma = 0.99, \quad n^u = 1, \quad N_x = 32, \quad M = 4, 8, 16, 32, 64.$$

5.3. Approximation of the trace operators. Next, we consider the Dirichlet trace operator $\mathcal{D}^u = \mathcal{D}^u(\varepsilon, \delta)$ and its Neumann counterpart $\mathcal{N}^u = \mathcal{N}^u(\varepsilon, \delta)$. In section 3 we saw that (c.f. (6)),

$$\mathcal{D}^u = \exp(gU), \quad \mathcal{N}^u = \exp(gU)U - (\partial_x g)\exp(gU)A,$$

and, in section 4.2, we posited the expansions

$$\{\mathcal{D}^u, \mathcal{N}^u\} = \{\mathcal{D}^u, \mathcal{N}^u\}(\varepsilon, \delta) = \sum_{n=0}^{\infty}\sum_{m=0}^{\infty}\left\{\mathcal{D}^u_{n,m}, \mathcal{N}^u_{n,m}\right\}\varepsilon^n\delta^m$$

(c.f. (18)), and recovered expressions for the HOPS/AWE terms $\{\mathcal{D}^u_{n,m}, \mathcal{N}^u_{n,m}\}$. As we have done in the previous two sections we simulate $\{\mathcal{D}^u, \mathcal{N}^u\}$ by the truncated Taylor series

$$\{\mathcal{D}^u, \mathcal{N}^u\} \approx \left\{\mathcal{D}^{u,N,M}, \mathcal{N}^{u,N,M}\right\}(\varepsilon, \delta) := \sum_{n=0}^{N}\sum_{m=0}^{M}\left\{\mathcal{D}^u_{n,m}, \mathcal{N}^u_{n,m}\right\}\varepsilon^n\delta^m. \tag{25}$$

Figure 4 shows the outcomes of the comparison between a numerical implementation of the approximation $\mathcal{D}^{u,N,M}$ (c.f. (25)), versus an exact computation of $\mathcal{D}^u$. More precisely we compute (at N_x collocation points on $[0, 2\pi]$)

$$\text{Error} := \frac{\left|\mathcal{D}^{u,N,M}(\varepsilon_{\max} f)[\xi] - \mathcal{D}^u(\varepsilon_{\max} f)[\xi]\right|_{L^\infty}}{\left|\mathcal{D}^u(\varepsilon_{\max} f)[\xi]\right|_{L^\infty}} \tag{26}$$

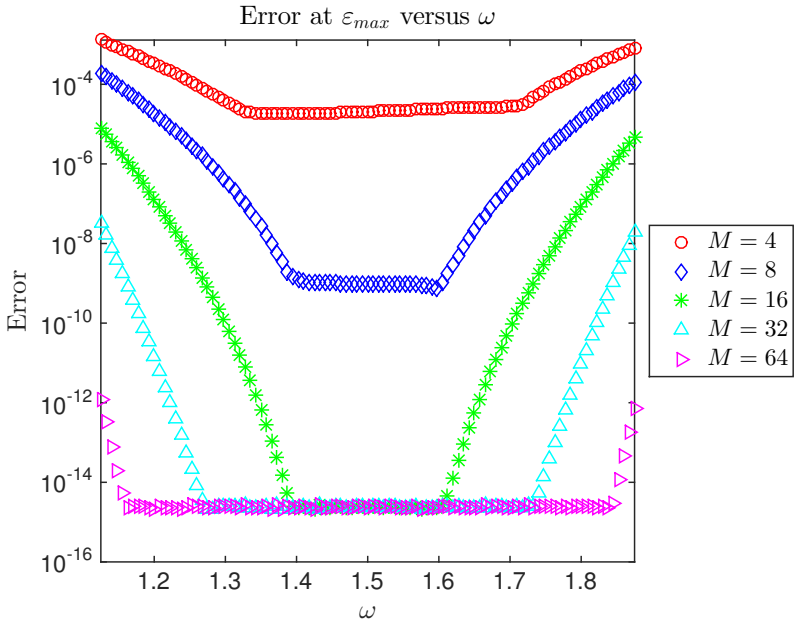

FIG. 4. *Relative supremum norm error,* (26)*, versus frequency* ω *in approximation of* $\mathcal{D}^u$ *by* $\mathcal{D}^{u,N,M}$ *for various perturbation orders* $N = M$*. Parameter choices are* $q = 1$*,* $\sigma = 0.99$*,* $n^u = 1$*,* $N_x = 32$*, and* $M = 4, 8, 16, 32, 64$*.*

for

$$\xi(x) = e^{\cos(x)} + ie^{\sin(x)}, \quad f(x) = \cos(x), \quad \varepsilon_{\max} = 0.2,$$

and parameter choices

$$q = 1, \quad \sigma = 0.99, \quad n^u = 1, \quad N_x = 32, \quad M = 4, 8, 16, 32, 64.$$

Figure 5 shows the outcomes of the comparison between a numerical implementation of the approximation $\mathcal{N}^{u,N,M}$ (c.f. (25)), versus an exact computation of $\mathcal{N}^u$. More precisely we compute (at N_x collocation points on $[0, 2\pi]$)

$$\text{Error} := \frac{\left|\mathcal{N}^{u,N,M}(\varepsilon_{\max} f)[\xi] - \mathcal{N}^u(\varepsilon_{\max} f)[\xi]\right|_{L^\infty}}{|\mathcal{N}^u(\varepsilon_{\max} f)[\xi]|_{L^\infty}} \tag{27}$$

for

$$\xi(x) = e^{\cos(x)} + ie^{\sin(x)}, \quad f(x) = \cos(x), \quad \varepsilon_{\max} = 0.2,$$

and parameter choices

$$q = 1, \quad \sigma = 0.99, \quad n^u = 1, \quad N_x = 32, \quad M = N = 4, 8, 16, 32, 64.$$

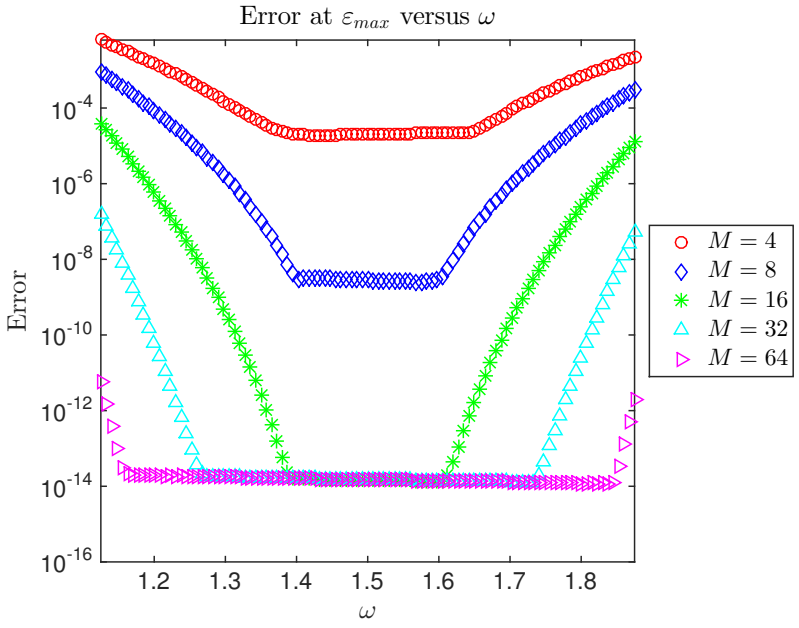

FIG. 5. *Relative supremum norm error,* (27)*, versus frequency* ω *in approximation of* $\mathcal{N}^u$ *by* $\mathcal{N}^{u,N,M}$ *for various perturbation orders* $N = M$*. Parameter choices are* $q = 1$*,* $\sigma = 0.99$*,* $n^u = 1$*,* $N_x = 32$*, and* $M = 4, 8, 16, 32, 64$*.*

5.4. Approximation of the reflectivity map. To close, we consider our original object of study, the reflectivity map $R = R(\varepsilon, \lambda)$, (3). Using both the FE recursions and their HOPS/AWE counterparts, we compute

$$R_{\text{FE}}^{N,N_x} \approx R, \quad R_{\text{HOPS/AWE}}^{N,M,N_x} \approx R,$$

and display, in Figure 6, the error

$$\text{Error} := \left| R_{\text{FE}}^{N,N_x} - R_{\text{HOPS/AWE}}^{N,M,N_x} \right|_{L^\infty} \tag{28}$$

for

$$f(x) = \cos(x), \quad \varepsilon_{\max} = 0.2,$$

and parameter choices

$$q = 1, \quad \sigma = 0.75, \quad n^u = 1, \quad n^w = 1.1, \quad N_x = 32, \quad M = N = 4, 8, 16, 32, 64.$$

We point out that $\sigma = 0.75$ was chosen in order to avoid the Rayleigh singularities coming from both the top *and* bottom layers.

To close this section we show the kind of simulations which our new HOPS/AWE method can produce with very high fidelity and quite modest computational effort. We revisit the calculations above in the cases $q = 1, 2, 3, 4, 5, 6$ with the following frequency and wavelength ranges ($\sigma = 0.99$):

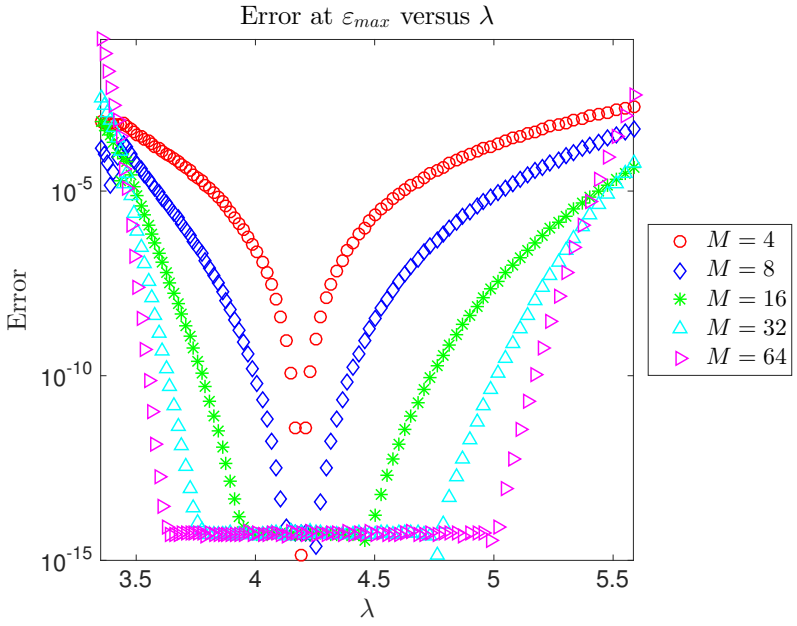

FIG. 6. *Relative supremum norm difference,* (28)*, between FE and HOPS/AWE algorithms versus wavelength* λ *in computation of the reflectivity map,* $R(\varepsilon_{max}, \lambda)$ *for various perturbation orders* $N = M$*. Parameter choices are* $q = 1$*,* $\sigma = 0.75$*,* $n^u = 1$*,* $n^w = 1.1$*,* $N_x = 32$*, and* $M = 4, 8, 16, 32, 64$*.*

$$
\begin{aligned}
q = 1: &\quad \omega \in [1.005, 1.995] &&\Longrightarrow &&\lambda \in [3.14947, 6.25193],\\
q = 2: &\quad \omega \in [2.005, 2.995] &&\Longrightarrow &&\lambda \in [2.09789, 3.13376],\\
q = 3: &\quad \omega \in [3.005, 3.995] &&\Longrightarrow &&\lambda \in [1.57276, 2.09091],\\
q = 4: &\quad \omega \in [4.005, 4.995] &&\Longrightarrow &&\lambda \in [1.25789, 1.56884],\\
q = 5: &\quad \omega \in [5.005, 5.995] &&\Longrightarrow &&\lambda \in [1.04807, 1.25538],\\
q = 6: &\quad \omega \in [6.005, 6.995] &&\Longrightarrow &&\lambda \in [0.89824, 1.04633].
\end{aligned}
$$

Once again we select

$$f(x) = \cos(x), \quad \varepsilon_{\max} = 0.2,$$

and parameter choices

$$n^u = 1, \quad n^w = 1.1, \quad N_x = 32, \quad M = N = 4.$$

In Figure 7(a) we plot the six "subsets" of the reflectivity map, R, all together on one set of axes. In Figure 7(b) we insert blue lines at the edges of the subsets showing how the entire approximation was built one piece at a time.

5.5. A rough interface. Finally, we consider the reflectivity map $R = R(\varepsilon, \lambda)$, (3), generated by a grating with a *rough* interface. In this setting we further validate our algorithm by making a comparison with the BIE solver for quasi-periodic gratings of Cho and Barnett [CB15] (see also the related work in [BG11, LKB15]). We mention that we are *greatly* indebted to both Barnett and Cho for not only providing us with an implementation [Bar16] of the algorithm in MATLAB [MAT10], but also for extensive

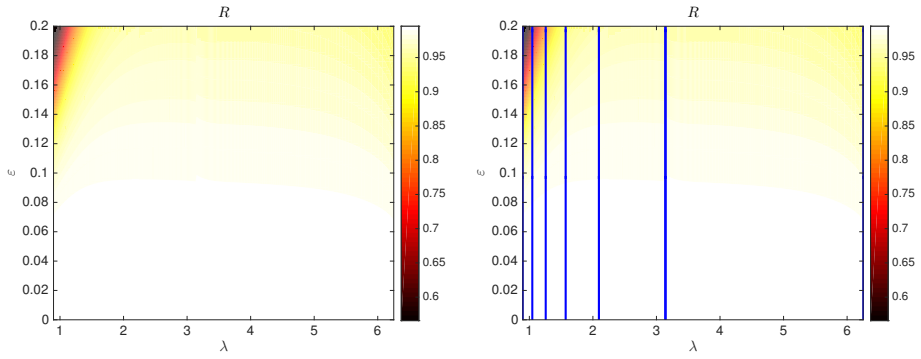

FIG. 7. *(a) The reflectivity map, $R(\varepsilon,\lambda)$, computed with six invocations of our new HOPS/AWE algorithm. Computed with $N = M = 4$ and a granularity of $N_\varepsilon = N_\delta = 101$ per invocation. Parameter choices are $\sigma = 0.99$, $n^u = 1$, $n^w = 1.1$, and $N_x = 32$. (b) Blue lines included to indicate boundaries between the six runs.*

assistance with its use. Now, using both the HOPS/AWE recursions and this BIE methodology we compute

$$R^{N_x}_{\text{BIE}} \approx R, \quad R^{N,M,N_x}_{\text{HOPS/AWE}} \approx R,$$

and display, in Figure 8, the error

$$\text{Error} := \left| R^{N_x}_{\text{BIE}} - R^{N,M,N_x}_{\text{HOPS/AWE}} \right|_{L^\infty} \tag{29}$$

for

$$f(x) = f_{L,P}(x) := \sum_{p=1}^{P} \frac{8}{\pi^2(2p-1)^2} \cos(2\pi p x), \quad P = 10, \quad \varepsilon_{\max} = 0.01, \quad d = 1,$$

and parameter choices

$$q = 1, \quad \sigma = 0.75, \quad n^u = 1, \quad n^w = 1.1, \quad N_x = 32, \quad M = N = 4, 8, 16, 32, 64.$$

(Here we have changed the period from 2π to 1 and the polarization from TM to TE to facilitate the BIE simulation.) The profile $f_{L,P}$ consists of the first P-many terms in a Fourier expansion of the Lipschitz profile

$$F_L(x) = \begin{cases} -4x + 1, & 0 \le x \le 1/2, \\ -3 + 4x, & 1/2 \le x \le 1. \end{cases}$$

Again, $\sigma = 0.75$ was chosen in order to avoid the Rayleigh singularities coming from both the top *and* bottom layers. In regards to Figure 8 we chose a discretization in the BIE algorithm ($N_x = 32$ quadrature points on the interface and along the fictitious boundaries; see [CB15] for more details) which had accuracy of approximately 10^{-12}.

5.6. Computational complexity. Of course the true motivation for this entire algorithm is the very advantageous computational complexity the HOPS/AWE approach has for computing quantities such as the reflectivity map, $R = R(\varepsilon,\lambda)$,

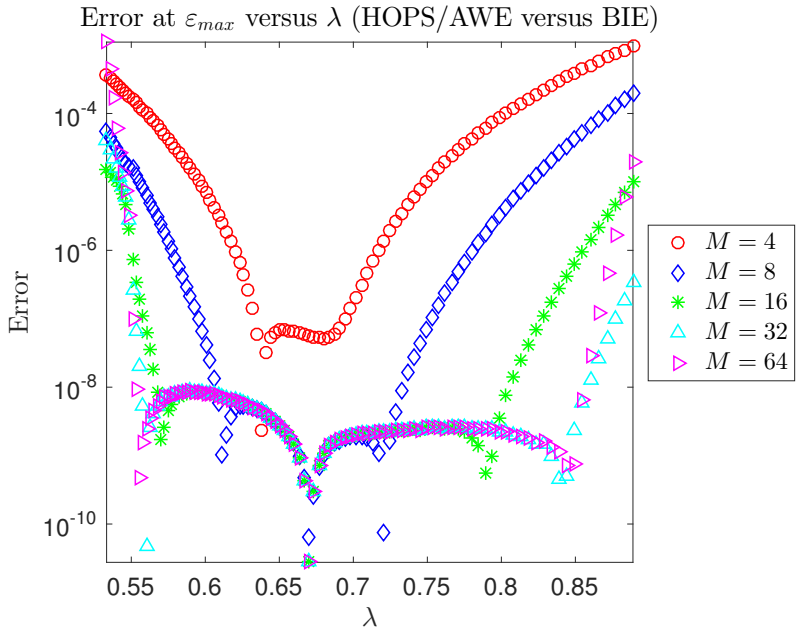

FIG. 8. *Relative supremum norm difference,* (29)*, between HOPS/AWE and BIE algorithms versus wavelength* λ *in computation of the reflectivity map,* $R(\varepsilon_{max}, \lambda)$ *for various perturbation orders* $N = M$*. Parameter choices are* $q = 1$*,* $\sigma = 0.75$*,* $n^u = 1$*,* $n^w = 1.1$*,* $N_x = 32$*, and* $M = 4, 8, 16, 32, 64$*.*

versus all other methods, even the highly efficient FE method. To summarize our conclusions on this front we begin by fixing the problem of computing R for N_ε many values of ε and N_δ many values of λ. Using any *surface* numerical method requires the use of a number of discretization points which we denote N_x. Finally, for the FE approach we will retain N perturbation orders in ε, while our new HOPS/AWE algorithm mandates the additional consideration of M Taylor orders in δ.

A careful study of the FE recursions (10) reveals that, for a single value of λ, *forming* the right-hand side at order n has cost

$$\mathcal{O}(nN_x \log(N_x)).$$

Inverting the operator $\mathbf{M}_0$ has complexity $\mathcal{O}(N_x \log(N_x))$ so that the full cost of computing the $\{a_{n,p}, d_{n,p}\}$ is therefore

$$\mathcal{O}(N^2 N_x \log(N_x)).$$

Once these are recovered, the cost of summing the series in ε is minimal, *provided* that it is done in an efficient manner (e.g., by Horner's rule [BF97, AH01]) so that the *full* cost of computing the reflectivity map by the FE method is

$$\mathcal{O}(N_\delta N^2 N_x \log(N_x)).$$

Consideration of the HOPS/AWE recursions (11) shows that the computational complexity in *forming* the right-hand side at order (n, m) has cost

$$\mathcal{O}(nmN_x \log(N_x)).$$

As before, inverting the operator $\mathbf{M}_{0,0}$ has complexity $\mathcal{O}(N_x \log(N_x))$ so that the full cost of computing the $\{a_{n,m,p}, d_{n,m,p}\}$ is therefore

$$\mathcal{O}(N^2 M^2 N_x \log(N_x)).$$

Again, once these coefficients are recovered, the cost of summing the series in (ε, δ) is minimal, *provided* that it is done in an efficient manner (e.g., by Horner's rule [BF97, AH01]) so that the *full* cost of computing the reflectivity map by the HOPS/AWE method is

$$\mathcal{O}(N^2 M^2 N_x \log(N_x)).$$

Thus, once $M^2 \ll N_\delta$ our new algorithm becomes prohibitively more efficient. Unsurprisingly this was a crucial consideration in the computations of section 5.4 as we often found $M = N = 4$ to be sufficient to produce the *entire* reflectivity map, while desiring a sampling of 100, 1000, or even 10,000 values in *both* the ε and λ variables.

6. Conclusion and future directions. In this paper we have described in some detail a novel, high-order spectral [GO77, CHQZ88] boundary/wavenumber perturbation method which, for problems akin to that of computing the reflectivity map, possesses optimal computational complexity and execution time. This HOPS/AWE algorithm has been shown to be both highly accurate and robust. However, it is clear that it can be extended and enhanced in a number of directions. In this concluding section we comment on some of these avenues which we intend to explore in forthcoming publications.

6.1. Three dimensions and vectorial scattering. To begin, it is trivial to see how our scheme could be extended to the three–dimensional problem of scattering of *scalar* waves by a two–dimensional periodic grating shaped by, e.g.,

$$z = g(x, y), \quad g(x + d_1, y + d_2) = g(x, y).$$

In short, every relevant formula from section 3 and section 4 would simply be modified by replacing occurrences of (αx) by $(\alpha x + \beta y)$ [MN11].

By contrast, two generalizations of interest to the author which are genuinely nontrivial are to the cases of *vectorial* scattering arising in electromagnetics [Jac75] and linear elastodynamics [Ach73], giving rise to Maxwell's and Navier's equations, respectively. In these situations (vector) Helmholtz equations (1a) and (1b) again govern the frequency-domain scattering while straightforward generalizations of quasi-periodicity and the outgoing wave condition are again relevant. The new complications come from the interfacial boundary conditions which are no longer as simple as (1c)–(1d). However, we have recently shown in the setting of Maxwell's equations [Nic15] how these conditions can be phrased in terms of trace operators akin to $\mathcal{D}^u$, $\mathcal{D}^w$, $\mathcal{N}^u$, and $\mathcal{N}^w$ resulting in equations much like (7)–(8). By expanding these operators (and those relevant to linear elastodynamics) in power series in ε and δ, it is easy to imagine how our HOPS/AWE approach could be readily extended to these important models.

6.2. Simulation of frequency-dependent materials. In this contribution we have focused exclusively upon materials whose index of refraction n (speed c) is both real and independent of ω. While the generalization to the setting where these constants take on imaginary values (e.g., for modeling the propagation of electromagnetic waves in a metal [Rae88, Mai07, EB12]) is straightforward, it will be interesting to

investigate the case where $n = n(\omega)$. Here we envision an index of refraction which can be expressed as a convergent Taylor series

$$n = n(\omega) = n(\underline{\omega} + \delta\underline{\omega}) = \sum_{m=0}^{\infty} n_m(\underline{\omega})\delta^m$$

in some disk $|\delta| < R$. In this case the dependence of $\{\mathcal{D}^u, \mathcal{D}^w, \mathcal{N}^u, \mathcal{N}^w\}$ upon δ will be more complicated and subtle; however, one can imagine that if the terms $\{\mathcal{D}^u_{n,m}, \mathcal{D}^w_{n,m}, \mathcal{N}^u_{n,m}, \mathcal{N}^w_{n,m}\}$ can be discovered, then a novel HOPS/AWE algorithm could be built.

6.3. Rayleigh singularity. To close, we reconsider the fundamental obstruction to the convergence of our algorithm: The Rayleigh singularities (Wood's anomalies)

$$\underline{\gamma}^u_p = 0 \quad \text{or} \quad \underline{\gamma}^w_p = 0 \quad \text{for } p \neq 0.$$

At this point it is unclear how to proceed in this setting to build a full HOPS/AWE algorithm, however, there is something we can say which may be the foundation for future developments. We now revisit the Taylor series expansion for γ^u_p of section 4.1 in the case $\underline{\gamma}^u_p = 0$. As expansion (12) is no longer valid (γ^u_p is *not* analytic in δ in this case) we seek a new form of "Puiseux type"

$$\gamma^u_p = \gamma^u_p(\delta) = \sum_{m=0}^{\infty} \gamma^u_{p,m}\delta^{m+1/2} = \delta^{1/2} \sum_{m=0}^{\infty} \gamma^u_{p,m}\delta^m \tag{30}$$

inspired by the fact that γ^u_p is the solution of a quadratic equation. Inserting this form into the relationship

$$\alpha_p^2 + (\gamma^u_p)^2 = (k^u)^2,$$

we find

$$\delta \left(\sum_{m=0}^{\infty} \gamma^u_{p,m}\delta^m \right) \left(\sum_{r=0}^{\infty} \gamma^u_{p,r}\delta^r \right) = (1+\delta)^2 (\underline{k}^u)^2 - \left(\underline{\alpha}_p + \delta\underline{\alpha}\right)^2.$$

This delivers

$$\begin{aligned} \delta \sum_{m=0}^{\infty} \delta^m \sum_{r=0}^{m} \gamma^u_{p,m-r}\gamma^u_{p,r} &= \left\{(\underline{k}^u)^2 - (\underline{\alpha}_p)^2\right\} + 2\delta \left\{(\underline{k}^u)^2 - \underline{\alpha}\ \underline{\alpha}_p\right\} + \delta^2 \left\{(\underline{k}^u)^2 - (\underline{\alpha})^2\right\} \\ &= 2\delta \left\{(\underline{k}^u)^2 - \underline{\alpha}\ \underline{\alpha}_p\right\} + \delta^2 (\underline{\gamma}^u)^2, \end{aligned}$$

where we have used that

$$(\underline{k}^u)^2 - (\underline{\alpha}_p)^2 = (\underline{\gamma}^u_p)^2 = 0.$$

Canceling a factor of δ, we find at order $\mathcal{O}(\delta^0)$

$$\gamma^u_{p,0} = \pm\sqrt{2((\underline{k}^u)^2 - \underline{\alpha}\ \underline{\alpha}_p)},$$

which we point out can *never* be zero. To see that this is true recall that $\underline{\gamma}_p^u = 0$ implies $(\underline{\alpha}_p)^2 = (\underline{k}^u)^2$ so

$$\gamma_{p,0}^u = \pm\sqrt{2((\underline{k}^u)^2 - \underline{\alpha}\,\underline{\alpha}_p)} = \pm\sqrt{2((\underline{\alpha}_p)^2 - \underline{\alpha}\,\underline{\alpha}_p)} = \pm\sqrt{2\underline{\alpha}_p}\sqrt{\alpha_p - \underline{\alpha}} \neq 0$$

since $p \neq 0$.

At order $\mathcal{O}(\delta^1)$ we require

$$\gamma_{p,1}^u = \frac{(\underline{\gamma}^u)^2}{2\gamma_{p,0}^u}, \quad \gamma_{p,0}^u \neq 0.$$

For $\mathcal{O}(\delta^m)$, $m > 1$, we demand

$$\gamma_{p,m}^u = \frac{-\sum_{r=1}^{m-1} \gamma_{p,m-r}^u \gamma_{p,r}^u}{2\gamma_{p,0}^u}, \quad \gamma_{p,0}^u \neq 0.$$

We now revisit the calculations of section 5.1 and produce the analogue of Figure 2 for the parameter choices

$$q = 3/2, \quad \sigma = 0.99, \quad n^u = 1, \quad N_x = 32, \quad M = 4, 8, 16, 32, 64$$

in the case $\delta > 0$. This delivers Figure 9 which displays the remarkable convergence and stability our Puiseux series can deliver. Given the Puiseux series (30) it is clear how one would approximate the operator U; however, how the trace operators, e.g., $\mathcal{D}^u$, would depend upon δ (the composition of an analytic function with a singular one) is unclear to the author.

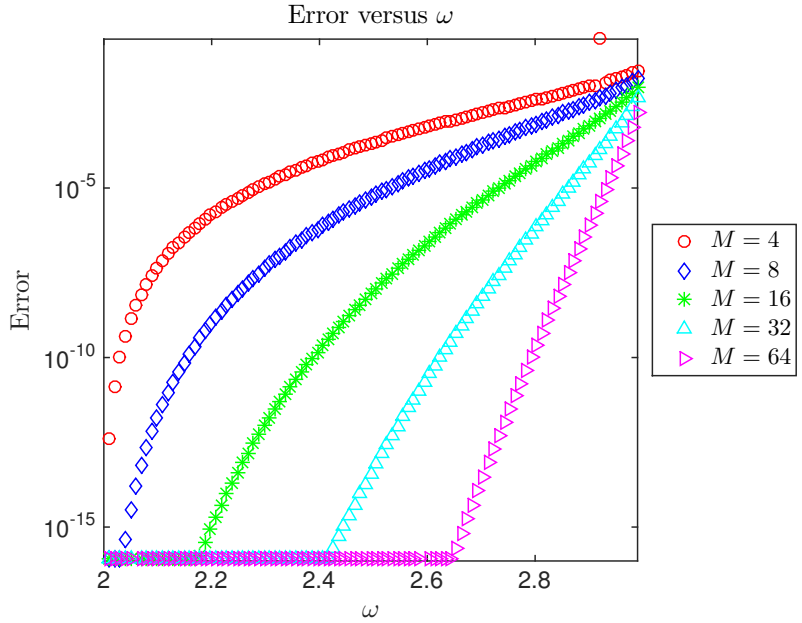

FIG. 9. *Relative supremum norm error,* (22)*, versus frequency* ω *in approximation of* γ_p^u *by* $\gamma_p^{u,M}$ $(N_x/2 \leq p \leq N_x/2 - 1)$ *for various perturbation orders* M*. Parameter choices are* $q = 3/2$*,* $\sigma = 0.99$*,* $n^u = 1$*,* $N_x = 32$*, and* $M = 4, 8, 16, 32, 64$

Acknowledgment. The author would like to thank F. Reitich for initial conversations and encouragement on this project. In addition to this, he pointed out the connection to the engineering literature, in particular, to that of the AWE.

REFERENCES

[Ach73] J. D. Achenbach, *Wave Propagation in Elastic Solids*, North–Holland, Amsterdam, 1973.

[AH01] K. Atkinson and W. Han, *Theoretical Numerical Analysis*, Texts Appl. Math. 39, Springer, New York, 2001.

[AN14] D. Ambrose and D. P. Nicholls, *Fokas integral equations for three dimensional layered–media scattering*, J. Comput. Phys., 276 (2014), pp. 1–25.

[Bar16] A. Barnett, *mpspack*, https://github.com/ahbarnett/mpspack (2016).

[BF97] R. Burden and J. D. Faires, *Numerical Analysis*, 6th ed., Brooks/Cole, Pacific Grove, CA, 1997.

[BG11] A. Barnett and L. Greengard, *A new integral representation for quasi-periodic scattering problems in two dimensions*, BIT, 51 (2011), pp. 67–90.

[BL82] L. M. Brekhovskikh and Y. P. Lysanov, *Fundamentals of Ocean Acoustics*, Springer, Berlin, 1982.

[BR93a] O. Bruno and F. Reitich, *Numerical solution of diffraction problems: A method of variation of boundaries*, J. Opt. Soc. Amer. A, 10 (1993), pp. 1168–1175.

[BR93b] O. Bruno and F. Reitich, *Numerical solution of diffraction problems: A method of variation of boundaries.* II. *Finitely conducting gratings, Padé approximants, and singularities*, J. Opt. Soc. Amer. A, 10 (1993), pp. 2307–2316.

[BR93c] O. Bruno and F. Reitich, *Numerical solution of diffraction problems: A method of variation of boundaries.* III. *Doubly periodic gratings*, J. Opt. Soc. Amer. A, 10 (1993), pp. 2551–2562.

[BR09] F. Bleibinhaus and S. Rondenay, *Effects of surface scattering in full-waveform inversion*, Geophysics, 74 (2009), pp. WCC69–WCC77.

[CB15] M. H. Cho and A. Barnett, *Robust fast direct integral equation solver for quasi–periodic scattering problems with a large number of layers*, Opt. Express, 23 (2015), pp. 1775–1799.

[CHQZ88] C. Canuto, M. Y. H, A. Quarteroni, and T. A. Zang, *Spectral Methods in Fluid Dynamics*, Springer, New York, 1988.

[CK98] D. Colton and R. Kress, *Inverse Acoustic and Electromagnetic Scattering Theory*, 2nd ed., Springer, Berlin, 1998.

[EB12] S. Enoch and N. Bonod, *Plasmonics: From Basics to Advanced Topics*, Springer Ser. Opt. Sci., Springer, New York, 2012.

[ELG98] T. W. Ebbesen, H. J. Lezec, H. F. Ghaemi, T. Thio, and P. A. Wolff, *Extraordinary optical transmission through sub-wavelength hole arrays*, Nature, 391 (1998), pp. 667–669.

[GO77] D. Gottlieb and S. A. Orszag, *Numerical Analysis of Spectral Methods: Theory and Applications*, CBMS-NSF Regional Conf. Ser. in Appl. Math. 26, SIAM, Philadelphia, 1977.

[God92] C. Godrèche, ed., *Solids Far from Equilibrium*, Cambridge University Press, Cambridge, 1992.

[GR87] L. Greengard and V. Rokhlin, *A fast algorithm for particle simulations*, J. Comput. Phys., 73 (1987), pp. 325–348.

[Hom08] J. Homola, *Surface plasmon resonance sensors for detection of chemical and biological species*, Chem. Rev., 108 (2008), pp. 462–493.

[ILW11] H. Im, S. H. Lee, N. J. Wittenberg, T. W. Johnson, N. C. Lindquist, P. Nagpal, D. J. Norris, and S.-H. Oh, *Template-stripped smooth Ag nanohole arrays with silica shells for surface plasmon resonance biosensing*, ACS Nano, 5 (2011), pp. 6244–6253.

[Jac75] J. D. Jackson, *Classical Electrodynamics*, 2nd ed., Wiley, New York, 1975.

[JJJ13] J. Jose, L. R. Jordan, T. W. Johnson, S. H. Lee, N. J. Wittenberg, and S.-H. Oh, *Topographically flat substrates with embedded nanoplasmonic devices for biosensing*, Adv. Funct. Mater, 23 (2013), pp. 2812–2820.

[KSN96] M. Kolbehdar, M. Srinivasan, M. Nakhla, Q.-J. Zhang , and R. Achar, *Simultaneous time and frequency domain solutions of EM problems using finite element and CFH techniques*, IEEE Trans. Microwave Theory Tech., 44 (1996), pp. 1526–1534.

[LJJ12] N. C. Lindquist, T. W. Johnson, J. Jose, L. M. Otto, and S.-H. Oh, *Ultrasmooth metallic films with buried nanostructures for backside reflection-mode plasmonic biosensing*, Ann. Phys., 524 (2012), pp. 687–696.

[LKB15] J. Lai, M. Kobayashi, and A. Barnett, *A fast and robust solver for the scattering from a layered periodic structure containing multi-particle inclusions*, J. Comput. Phys., 298 (2015), pp. 194–208.

[Mai07] S. A. Maier, *Plasmonics: Fundamentals and Applications*, Springer, New York, 2007.

[MAT10] The MathWorks Inc., MATLAB, *version* 7.10.0 *(R*2010*a)*, Natick, MA, 2010.

[MN11] A. Malcolm and D. P. Nicholls, *A field expansions method for scattering by periodic multilayered media*, J. Acoust. Soc. Amer., 129 (2011), pp. 1783–1793.

[Mos85] M. Moskovits, *Surface–enhanced spectroscopy*, Rev. Modern Phys., 57 (1985), pp. 783–826.

[MR87] T. R. Marchant and A. J. Roberts, *Properties of short-crested waves in water of finite depth*, J. Austr. Math. Soc. Ser. B, 29 (1987), pp. 103–125.

[Nic12] D. P. Nicholls, *Three–dimensional acoustic scattering by layered media: A novel surface formulation with operator expansions implementation*, R. Soc. Lond. Proc. Ser. A Math. Phys. Eng. Sci., 468 (2012), pp. 731–758.

[Nic15] D. P. Nicholls, *A method of field expansions for vector electromagnetic scattering by layered periodic crossed gratings*, J. Opt. Soc. Amer. A, 32 (2015), pp. 701–709.

[Nic16] D. P. Nicholls, *A high–order perturbation of surfaces (HOPS) approach to Fokas integral equations: Three–dimensional layered media scattering*, Quart. Appl. Math., 74 (2016), pp. 61–87.

[NOJR16] D. P. Nicholls, S.-H. Oh, T. W. Johnson, and F. Reitich, *Launching surface plasmon waves via vanishingly small periodic gratings*, J. Opt. Soc. Amer. A, 33 (2016), pp. 276–285.

[NR01] D. P. Nicholls and F. Reitich, *A new approach to analyticity of Dirichlet-Neumann operators*, Proc. Roy. Soc. Edinburgh Sect. A, 131 (2001), pp. 1411–1433.

[NR03] D. P. Nicholls and F. Reitich, *Analytic continuation of Dirichlet-Neumann operators*, Numer. Math., 94 (2003), pp. 107–146.

[NR04a] D. P. Nicholls and F. Reitich, *Shape deformations in rough surface scattering: Cancellations, conditioning, and convergence*, J. Opt. Soc. Amer. A, 21 (2004), pp. 590–605.

[NR04b] D. P. Nicholls and F. Reitich, *Shape deformations in rough surface scattering: Improved algorithms*, J. Opt. Soc. Amer. A, 21 (2004), pp. 606–621.

[NR08] D. P. Nicholls and F. Reitich, *Boundary perturbation methods for high–frequency acoustic scattering: Shallow periodic gratings*, J. Acoust. Soc. Amer., 123 (2008), pp. 2531–2541.

[NRJO14] D. P. Nicholls, F. Reitich, T. W. Johnson, and S.-H. Oh, *Fast high–order perturbation of surfaces (HOPS) methods for simulation of multi–layer plasmonic devices and metamaterials*, J. Opt. Soc. Amer. A, 31 (2014), pp. 1820–1831.

[NT16] D. P. Nicholls and V. Tammali, *A high–order perturbation of surfaces (HOPS) approach to Fokas integral equations: Vector electromagnetic scattering by periodic crossed gratings*, Appl. Numer. Methods, 101 (2016), pp. 1–17.

[NW01] F. Natterer and F. Wübbeling, *Mathematical Methods in Image Reconstruction*, Math. Model. Comput., SIAM, Philadelphia, 2001.

[Pet80] R. Petit, ed., *Electromagnetic Theory of Gratings*, Springer, Berlin, 1980.

[Pou84] M. Pourahmadi, *Taylor expansion of* $\exp(\sum_{k=0}^{\infty} a_k z^k)$ *and some applications*, Amer. Math. Monthly, 91 (1984), pp. 303–307.

[PR90] L. Pillage and R. Rohrer, *Asymptotic waveform evaluation for timing analysis*, IEEE Trans. Comput.-Aided Des., 9 (1990), pp. 352–366.

[Rae88] H. Raether, *Surface Plasmons on Smooth and Rough Surfaces and on Gratings*, Springer, Berlin, 1988.

[Ray07] L. Rayleigh, *On the dynamical theory of gratings*, R. Soc. Lond. Proc. Ser. A Math. Phys. Eng. Sci., A, 79 (1907), pp. 399–416.

[RDCB98] C. J. Reddy, M. D. Deshpande, C. R. Cockrell, and F. B. Beck, *Fast RCS computation over a frequency band using method of moments in conjunction with asymptotic waveform evaluation technique*, IEEE Trans. Antennas and Propagation, 46 (1998), pp. 1229–1233.

[Ric51] S. O. Rice, *Reflection of electromagnetic waves from slightly rough surfaces*, Comm. Pure Appl. Math., 4 (1951), pp. 351–378.

[RJOM13] F. Reitich, T. W. Johnson, S.-H. Oh, and G. Meyer, *A fast and high-order accurate boundary perturbation method for characterization and design in nanoplasmonics*, J. Opt. Soc. Amer. A, 30 (2013), pp. 2175–2187.

[Rob83] A. J. Roberts, *Highly nonlinear short-crested water waves*, J. Fluid Mech., 135 (1983), pp. 301–321.

[RT04] F. Reitich and K. Tamma, *State–of–the–art, trends, and directions in computational electromagnetics*, CMES Comput. Model. Eng. Sci., 5 (2004), pp. 287–294.

[SLL01] R. Sloane, R. Lee, and J.-F. Lee, *Multipoint Galerkin asymptotic waveform evaluation for model order reduction of frequency domain FEM electromagnetic radiation problems*, IEEE Trans. Antennas and Propagation, 49 (2001), pp. 1504–1513.

[VO09] J. Virieux and S. Operto, *An overview of full-waveform inversion in exploration geophysics*, Geophysics, 74 (2009), pp. WCC1–WCC26.